Current Biology, Volume *27*

Supplemental Information

BubR1 Promotes Bub3-Dependent APC/C Inhibition during Spindle Assembly Checkpoint Signaling

Katharina Overlack, Tanja Bange, Florian Weissmann, Alex C. Faesen, Stefano Maffini, Ivana Primorac, Franziska Müller, Jan-Michael Peters, and Andrea Musacchio

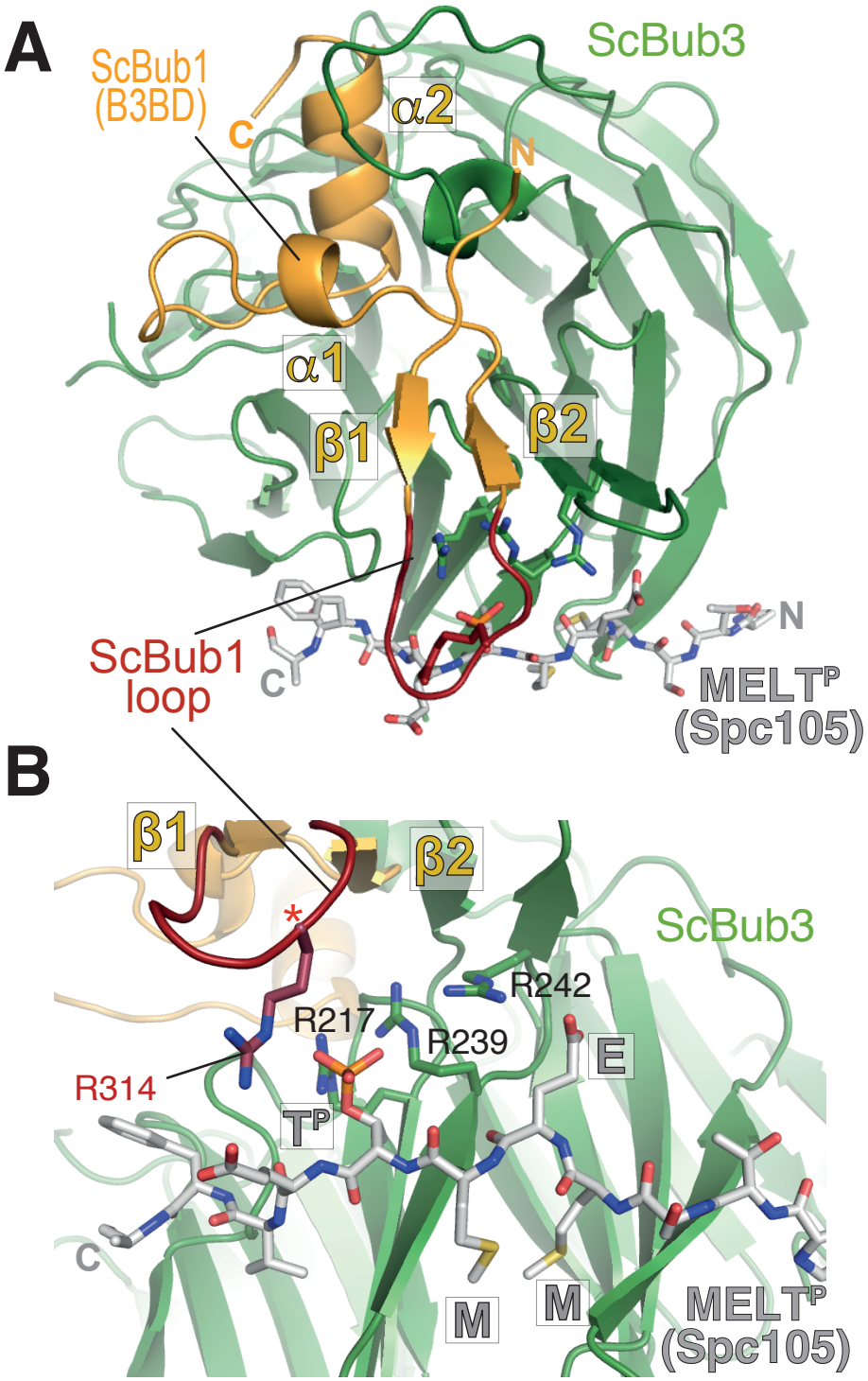
A
ScBub1
(B3BD)
C
α2
N
ScBub3
α1
β1
β2
ScBub1
loop
C
N
MELTP
(Spc105)
B
β1
β2
*
ScBub3
R242
R217
R239
E
R314
TP
C
M
M
MELTP
(Spc105)

Figure S1 ***Crystal structure of the Bub1-Bub3-MELT^{P} ternary complex*****. Related to Figure 1**

A) Crystal structure of the Bub1$^{289-359}$-Bub3-MELT^{P} ternary complex from *S. cerevisiae* (Sc) [S1]. N and C indicate the N- and C-terminus, respectively. **B**) Close-up of the MELT^{P} binding site indicating the role of ScBub1^{R314} in MELT^{P} binding. The two panels are reproduced from panels C and D of Figure 2 in [S2].

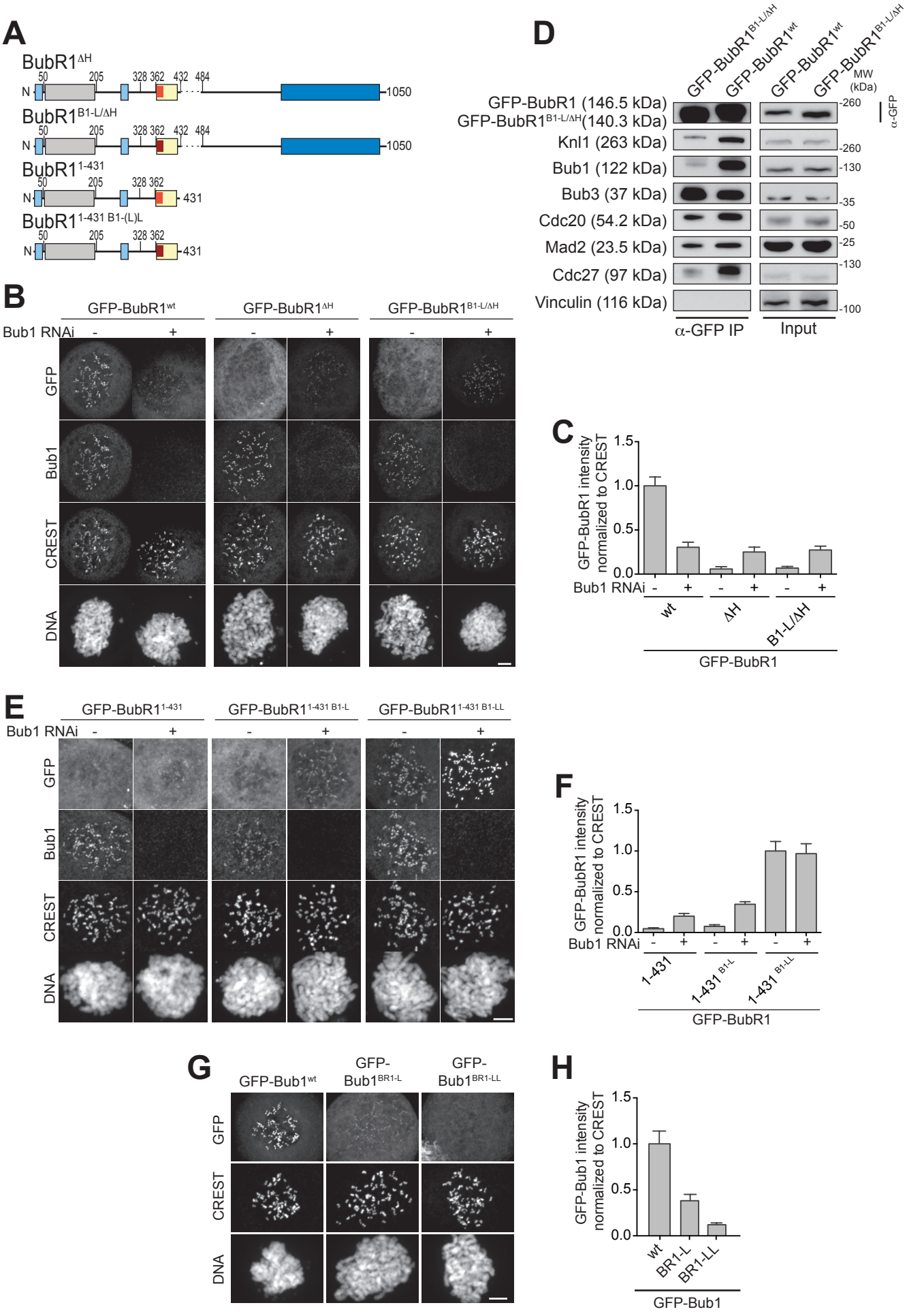
A
BubR1ΔH
BubR1B1-L/ΔH
BubR1 1-431
BubR1 1-431 B1-(L)L
N
50
205
328 362
432 484
1050
431
B
GFP-BubR1wt
GFP-BubR1ΔH
GFP-BubR1B1-L/ΔH
Bub1 RNAi
GFP
Bub1
CREST
DNA
C
GFP-BubR1 intensity normalized to CREST
wt
ΔH
B1-L/ΔH
GFP-BubR1
D
GFP-BubR1 (146.5 kDa)
GFP-BubR1B1-L/ΔH(140.3 kDa)
Knl1 (263 kDa)
Bub1 (122 kDa)
Bub3 (37 kDa)
Cdc20 (54.2 kDa)
Mad2 (23.5 kDa)
Cdc27 (97 kDa)
Vinculin (116 kDa)
MW (kDa)
α-GFP
α-GFP IP
Input
E
GFP-BubR1 1-431
GFP-BubR1 1-431 B1-L
GFP-BubR1 1-431 B1-LL
F
1-431
1-431 B1-L
1-431 B1-LL
G
GFP-Bub1wt
GFP-Bub1BR1-L
GFP-Bub1BR1-LL
H
GFP-Bub1 intensity normalized to CREST
wt
BR1-L
BR1-LL
GFP-Bub1

Figure S2 ***Definition of functional loop regions of Bub1and BubR1.*** **Related to Figure 1**

A) Domain organization of the BubR1 mutants used in this figure. **B**, **E**) Representative images of HeLa cells transfected with the indicated GFP-BubR1 constructs show that the short Bub1 loop (B1-L) is not sufficient to rescue kinetochore localization of $BubR1^{\Delta H}$ (B) or $BubR1^{1-431}$ (first four columns panel E). This experiment aimed to test the prediction that after being grafted $Bub1^{L}$, BubR1 can localize to kinetochores independently of Bub1. The 432-484 region of BubR1 is required for its dimerization with Bub1 and is required for kinetochore recruitment of BubR1 [S2]. We expected this region to become dispensable for kinetochore localization after grafting of $Bub1^{L}$. Contrary to this expectation, however, when we combined grafting of $Bub1^{L}$ with deletion of residues 432-484 in the predicted helical region of BubR1 ($BubR1^{B1\text{-}L/\Delta H}$; see panel A and Introduction), we found that GFP-$BubR1^{B1\text{-}L/\Delta H}$ was unable to localize to kinetochores, regardless of whether endogenous Bub1 had been depleted or not (panels B-C). This was not due to a reduced interaction of the GFP-$BubR1^{B1\text{-}L/\Delta H}$ mutant with Bub3 in comparison to GFP-$BubR1^{wt}$ (see panel D). We reasoned that deletion of the BubR1 helical domain in GFP-$BubR1^{B1\text{-}L/\Delta H}$ might unleash a hypothetical intra-molecular regulatory mechanism – based on sequences downstream of the helical domain – designed to suppress BubR1 kinetochore recruitment. However, the observation that grafting of $Bub1^{L}$ also fails to promote kinetochore localization of $BubR1^{1-431}$ ($BubR1^{1\text{-}431/B1\text{-}L}$), a truncation construct impaired in the interaction with Bub1 (because truncated before the predicted helical domain; Panels A and E-F), excluded this possibility. Thus, GFP-$BubR1^{B1\text{-}L}$ continues to depend on the helical domain for kinetochore recruitment. It is likely that the BubR1 helical domain contributes to kinetochore localization by binding, in addition to Bub1, also to another kinetochore receptor (because GFP-$BubR1^{B1\text{-}L}$ localizes to kinetochores also in the absence of Bub1 [S2]), a possibility that we are currently addressing. Because the B3BD of Bub1 is fully sufficient for kinetochore recruitment through Bub3 [S2-S4], we hypothesized that our failure to fully recapitulate this property in our grafting experiments may depend on an imperfect choice of the Bub1 sequence grafted onto BubR1. Indeed, the long loop (B1-LL) can rescue kinetochore localization of $BubR1^{1-431}$ (last two columns panel E). For panels B and E, cells were treated as in Figure 1E. Scale bar: 10 μm. **C**, **F**) Quantification of BubR1 kinetochore levels in cells treated as in B and E, respectively. The graphs show mean

intensity from three independent experiments. Error bars represent SEM. Values for $BubR1^{wt}$ or $BubR1^{1\text{-}431\ B1\text{-}LL}$ in non-depleted cells are set to 1, respectively. **D**) Western Blot of immunoprecipitates (IP) from mitotic Flp-In T-REx cell lines expressing the indicated GFP-BubR1 constructs showing that $BubR1^{B1\text{-}L/_{\Delta}H}$ binds similar amounts of Bub3 as $BubR1^{wt}$. Vinculin was used as loading control. **G**) Representative images of HeLa cells transfected with the indicated GFP-Bub1 constructs showing that GFP-$Bub1^{BR1\text{-}LL}$ is more strongly impaired in kinetochore localization than the short loop mutant (BR1-L). Scale bar: 10 μm. **H**) Quantification of Bub1 kinetochore levels in cells treated as in G. The graph shows mean intensity from three independent experiments. Error bars represent SEM. Values for $Bub1^{wt}$ are set to 1.

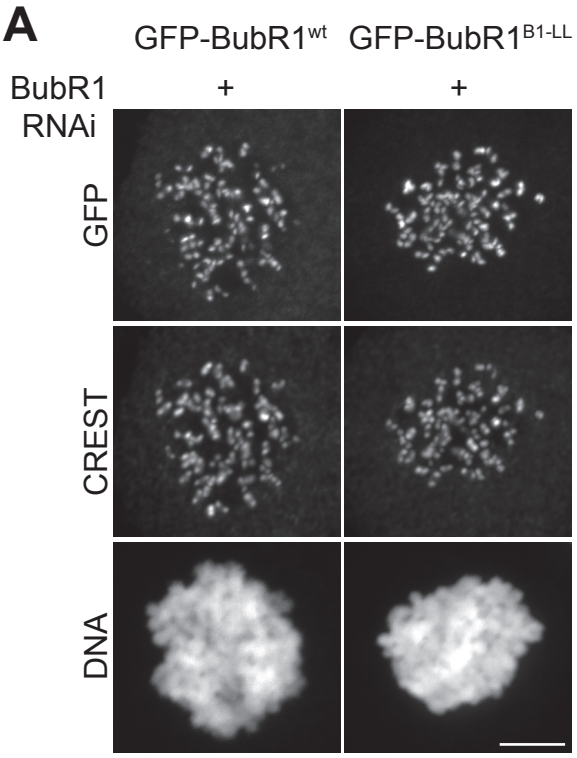
A
GFP-BubR1wt
GFP-BubR1B1-LL
BubR1 RNAi
+
+
GFP
CREST
DNA
B
GFP-BubR1 intensity normalized to CREST
2.0
1.5
1.0
0.5
0.0
BubR1 RNAi
+
+
wt
B1-LL
GFP-BubR1

Figure S3 ***GFP-BubR1$^{B1\text{-}LL}$ levels in BubR1 RNAi.*** **Related to Figure 1**

A) Representative images of stable Flp-In T-REx stable cell lines expressing the indicated GFP-BubR1 constructs in the absence of endogenous BubR1. **B**) Quantification of GFP-BubR1 kinetochore levels expressing the indicated GFP-BubR1 constructs treated as in **A**. The graph shows mean intensity from three independent experiments. Error bars represent SEM. Values for GFP-BubR1^{wt} are set to 1.

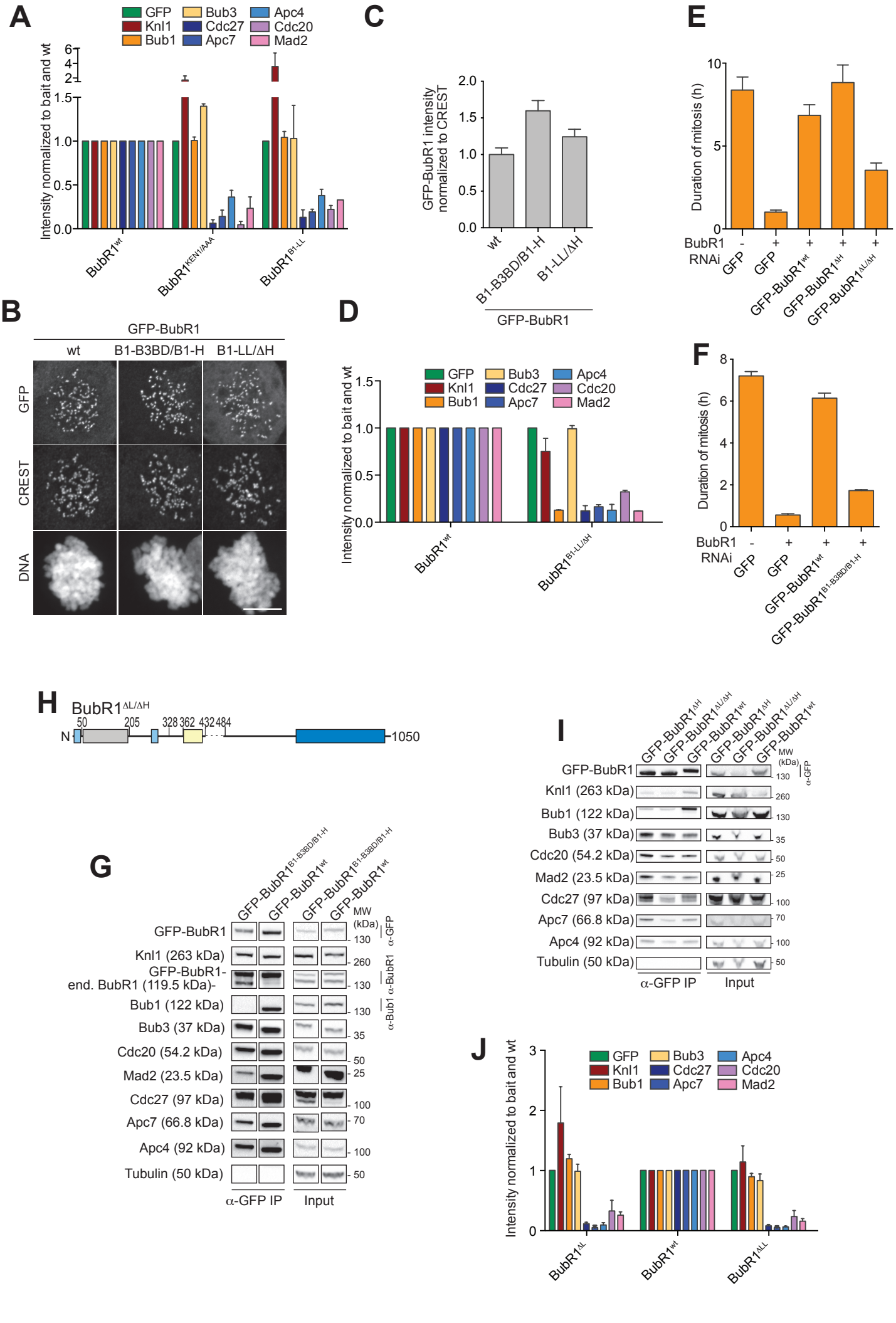
A
GFP
Knl1
Bub1
Bub3
Cdc27
Apc7
Apc4
Cdc20
Mad2
Intensity normalized to bait and wt
BubR1wt
BubR1KEN1/AAA
BubR1B1-LL
B
GFP-BubR1
wt
B1-B3BD/B1-H
B1-LL/ΔH
GFP
CREST
DNA
C
GFP-BubR1 intensity normalized to CREST
wt
B1-B3BD/B1-H
B1-LL/ΔH
GFP-BubR1
D
Intensity normalized to bait and wt
BubR1wt
BubR1B1-LL/ΔH
E
Duration of mitosis (h)
BubR1 RNAi
GFP
GFP-BubR1wt
GFP-BubR1ΔH
GFP-BubR1ΔL/ΔH
F
Duration of mitosis (h)
BubR1 RNAi
GFP
GFP-BubR1wt
GFP-BubR1B1-B3BD/B1-H
H
BubR1ΔL/ΔH
N
50
205
328
362
432
484
1050
I
GFP-BubR1
Knl1 (263 kDa)
Bub1 (122 kDa)
Bub3 (37 kDa)
Cdc20 (54.2 kDa)
Mad2 (23.5 kDa)
Cdc27 (97 kDa)
Apc7 (66.8 kDa)
Apc4 (92 kDa)
Tubulin (50 kDa)
MW (kDa)
α-GFP
α-GFP IP
Input
G
GFP-BubR1
Knl1 (263 kDa)
GFP-BubR1-end. BubR1 (119.5 kDa)-
Bub1 (122 kDa)
Bub3 (37 kDa)
Cdc20 (54.2 kDa)
Mad2 (23.5 kDa)
Cdc27 (97 kDa)
Apc7 (66.8 kDa)
Apc4 (92 kDa)
Tubulin (50 kDa)
MW (kDa)
α-GFP
α-Bub1
α-GFP IP
Input
J
Intensity normalized to bait and wt
BubR1ΔL
BubR1wt
BubR1ΔLL

Figure S4 ***The BubR1-loop is required for BubR1 SAC function in vivo.*** **Related to Figures 2, 3, and 6.**

A, **D**) Quantification of the Western Blots in Figure 2C and Figure 2G, respectively. The amounts of co-precipitating proteins were normalized to the amount of GFP-BubR1 bait present in the IP. Values for GFP-BubR1^{wt} are set to 1. The graphs show mean intensity of at least two independent experiments. Error bars represent SEM. **B**) Representative images of Flp-In T-REx stable cell lines expressing the indicated GFP-BubR1 constructs showing kinetochore localization, as expected. Scale bar: 10 μm. **C**) Quantification of BubR1 kinetochore levels in cells treated as in B. The graph shows mean intensity from at least two independent experiments. Error bars represent SEM. Values for BubR1^{wt} are set to 1. **E**, **F**) Mean duration of mitosis of Flp-In T-REx stable cell lines expressing the indicated GFP-BubR1 constructs in the absence of endogenous BubR1 and in the presence of 50 nM nocodazole. Cell morphology was used to measure entry into and exit from mitosis by time-lapse-microscopy (n>25 for BubR1$^{\Delta H}$ and BubR1$^{\Delta L/\Delta H}$ (E), n>20 for BubR1$^{B1\text{-}B3BD/B1\text{-}H}$ (F) per cell line per experiment) from at least two independent experiments. Error bars depict SEM. **G**) Western blot of IPs from mitotic Flp-In T-REx cell lines expressing the indicated GFP-BubR1 constructs and showing that BubR1$^{B1\text{-}B3BD/B1\text{-}H}$ is impaired in APC/C binding. Intervening lanes of different samples have been cropped. Note that that reduced but still significant levels of APC/C binding visible here are due to the ability of this construct to bind endogenous BubR1, which was not depleted in this experiment, and which is clearly visible in the IPs. **H**) Domain organization of the BubR1 construct lacking the loop and the helix. **I**) Western Blots of immunoprecipitates (IP) from mitotic Flp-In T-REx cell lines expressing the indicated GFP-BubR1 constructs showing that the deletion of the loop results in impaired APC/C binding also of BubR1$^{\Delta H}$. Tubulin was used as loading control. **J**) Quantification of Western blot in Figure 3F. The amounts of co-precipitating proteins were normalized to the amount of GFP-BubR1 bait present in the IP. Values for GFP-BubR1^{wt} are set to 1. The graph shows mean intensity of two independent experiments. Error bars represent SEM.

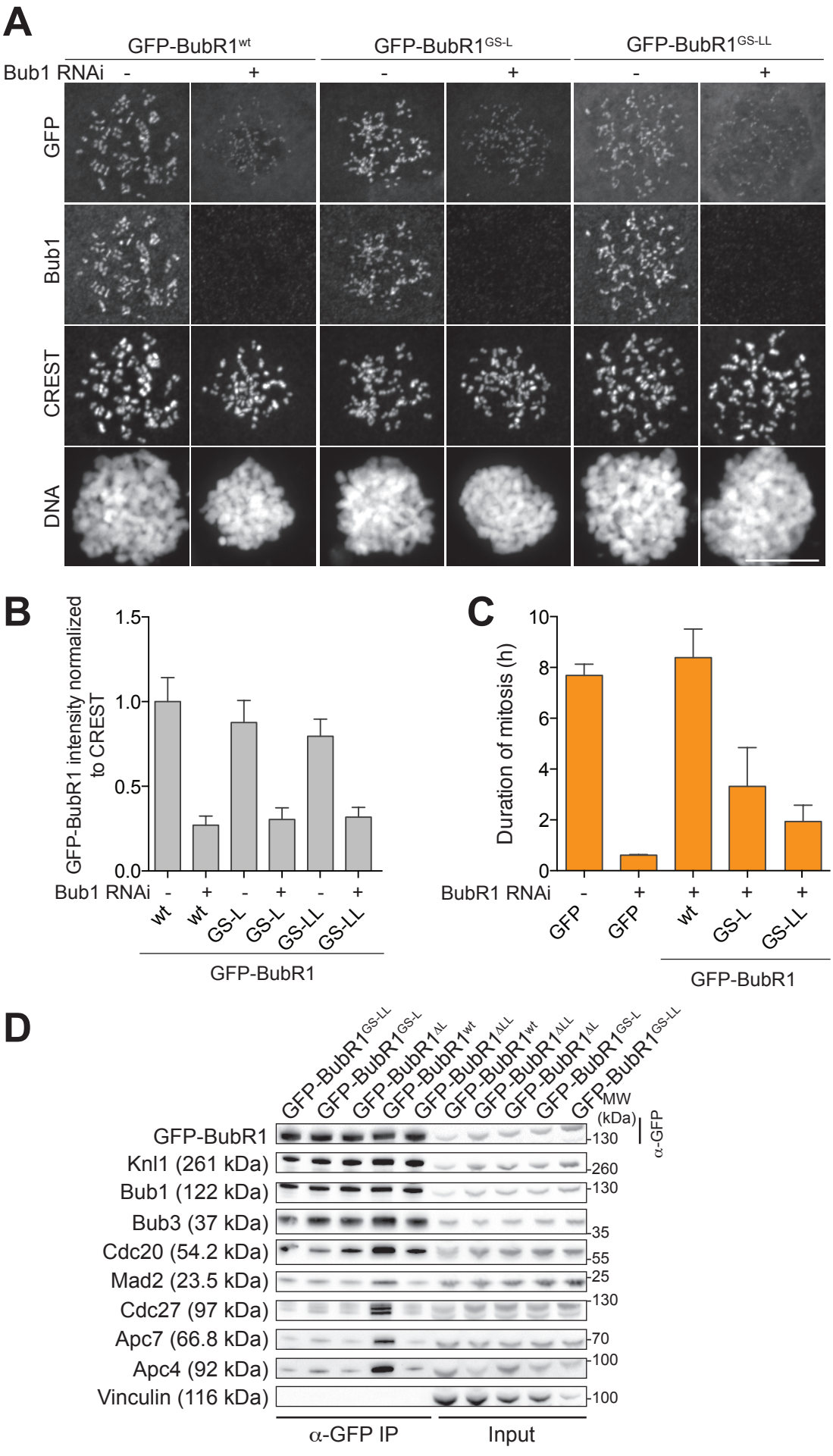
A
GFP-BubR1wt
GFP-BubR1GS-L
GFP-BubR1GS-LL
Bub1 RNAi - + - + - +
GFP
Bub1
CREST
DNA
B
GFP-BubR1 intensity normalized to CREST
1.5
1.0
0.5
0.0
Bub1 RNAi - + - + - +
wt wt GS-L GS-L GS-LL GS-LL
GFP-BubR1
C
Duration of mitosis (h)
10
8
6
4
2
0
BubR1 RNAi - + + + +
GFP GFP wt GS-L GS-LL
GFP-BubR1
D
GFP-BubR1GS-LL
GFP-BubR1GS-L
GFP-BubR1ΔL
GFP-BubR1wt
GFP-BubR1ΔLL
GFP-BubR1wt
GFP-BubR1ΔLL
GFP-BubR1ΔL
GFP-BubR1GS-L
GFP-BubR1GS-LL
MW (kDa)
α-GFP
GFP-BubR1
Knl1 (261 kDa)
Bub1 (122 kDa)
Bub3 (37 kDa)
Cdc20 (54.2 kDa)
Mad2 (23.5 kDa)
Cdc27 (97 kDa)
Apc7 (66.8 kDa)
Apc4 (92 kDa)
Vinculin (116 kDa)
130
260
130
35
55
25
130
70
100
100
α-GFP IP
Input

Figure S5 ***Behavior of "neutral" (GS) loop mutants of Bub****R1****.*** **Related to Figure 2**

A) Representative images of HeLa cells transfected with the indicated GFP-BubR1 constructs in presence or absence of endogenous Bub1 showing that the replacement of the loop with a neutral GS-sequence does not influence kinetochore localization, as expected. Cells were treated as in Figure 1E. Scale bar: 10 μm. **B**) Quantification of GFP-BubR1 kinetochore levels in cells treated as in A. The graph shows mean intensity from three independent experiments. Error bars represent SEM. Values for $BubR1^{wt}$ in non-depleted cells are set to 1. **C**) Mean duration of mitosis of Flp-In T-REx stable cell lines expressing the indicated GFP-BubR1 constructs in the absence of endogenous BubR1 and in the presence of 50 nM nocodazole. Cell morphology was used to measure entry into and exit from mitosis by time-lapse-microscopy (n>32 for BubR1GS-(L)L per cell line per experiment) from two independent experiments. Error bars indicate SEM. **D**) Western Blot of immunoprecipitates (IP) from mitotic Flp-In T-REx cell lines expressing the indicated GFP-BubR1 constructs showing that replacement of the loop with a neutral GS-sequence as the lack of the loop result in strongly impaired APC/C binding. Vinculin was used as loading control. Note that a part of this blot is already shown in Figure 3F.

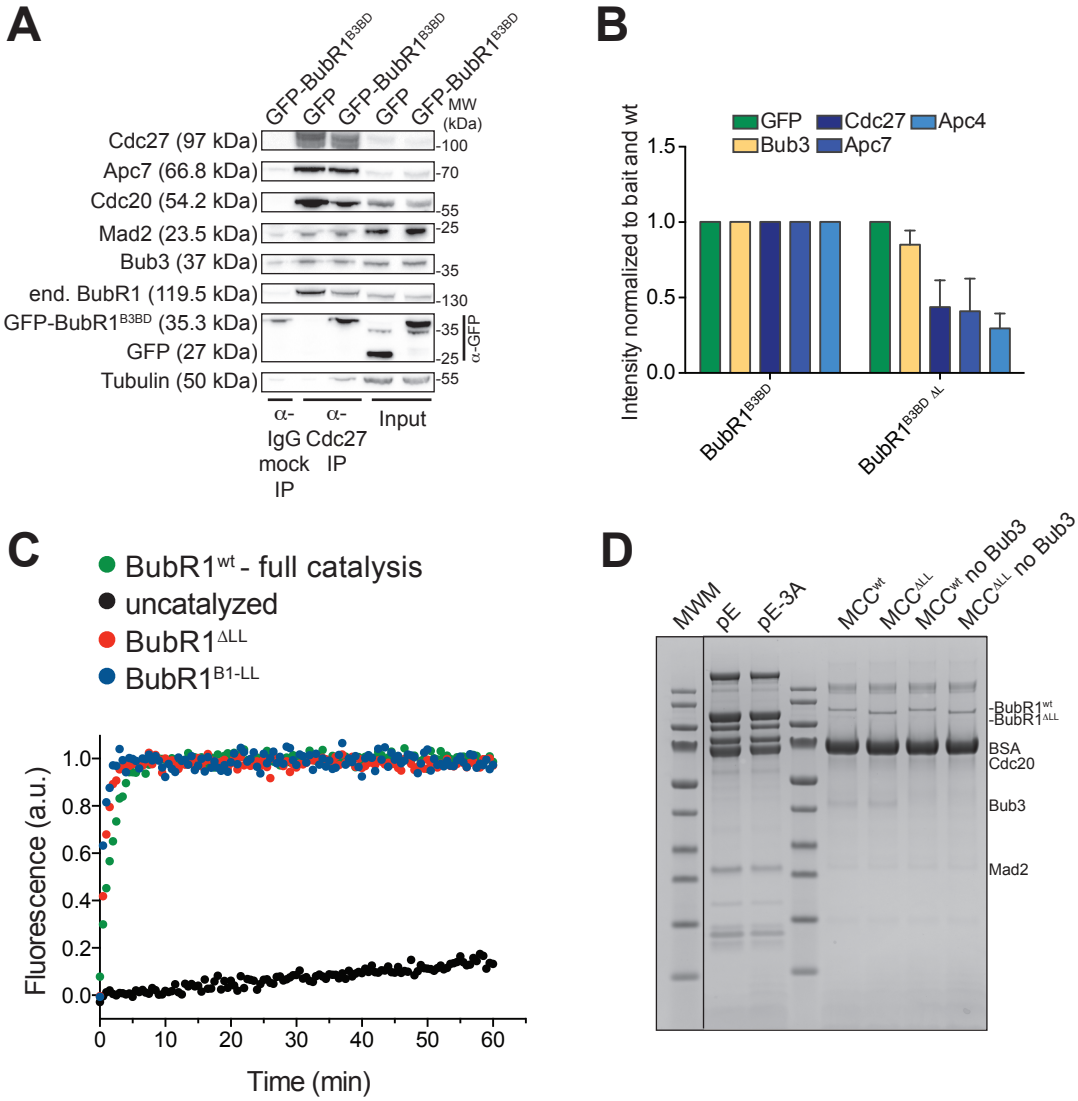
A
GFP-BubR1B3BD
GFP
GFP-BubR1B3BD
GFP
GFP-BubR1B3BD
MW (kDa)
Cdc27 (97 kDa)
Apc7 (66.8 kDa)
Cdc20 (54.2 kDa)
Mad2 (23.5 kDa)
Bub3 (37 kDa)
end. BubR1 (119.5 kDa)
GFP-BubR1B3BD (35.3 kDa)
GFP (27 kDa)
Tubulin (50 kDa)
-100
-70
-55
-25
-35
-130
-35
-25
-55
α-GFP
α-IgG mock IP
α-Cdc27 IP
Input
B
GFP
Cdc27
Apc4
Bub3
Apc7
Intensity normalized to bait and wt
1.5
1.0
0.5
0.0
BubR1B3BD
BubR1B3BD ΔL
C
BubR1wt - full catalysis
uncatalyzed
BubR1ΔLL
BubR1B1-LL
Fluorescence (a.u.)
1.0
0.8
0.6
0.4
0.2
0.0
0
10
20
30
40
50
60
Time (min)
D
MWM
pE
pE-3A
MCCwt
MCCΔLL
MCCwt no Bub3
MCCΔLL no Bub3
BubR1wt
BubR1ΔLL
BSA
Cdc20
Bub3
Mad2
E
no APC/C
pE
pE-3A
APC/C (20 nM)
no MCC
WT
ΔLL
no MCC
WT
ΔLL
MCC (30 nM)
120 30 60 120 30 60 120 30 60 120 30 60 120 30 60 120 30 60 120
Time (min)
CycBNTD*-Ubn
CycBNTD*

Figure S6 ***The BubR1-loop promotes APC/C binding.*** **Related to Figures 4 and 5.**

A) Western Blot of α-Cdc27 immunoprecipitates (IP) from mitotic Flp-In T-REx cell lines expressing either GFP or GFP-BubR1^{B3BD} showing that the B3BD of BubR1 is pulled down with the APC/C. Tubulin was used as loading control. The background binding detected in the IgG mock IP is presumably due to low stringency washes. **B**) Quantification of the Western Blot in Figure 4D. The amounts of co-precipitating proteins were normalized to the amount of GFP-BubR1 bait present in the IP. Values for GFP-BubR1^{B3BD} are set to 1. The graph shows mean intensity of two independent experiments. Error bars represent SEM. **C**) Assembly kinetics of MCC complexes containing the BubR1 loop mutants are the same as for MCC complexes containing BubR1^{wt}. The assay was performed as described in [S5]. The curve is representative of three replicates. a.u., arbitrary units. **D**) Coomassie-stained SDS-PAGE of pooled samples of different MCC and APC/C complexes after gel filtration. MWM, molecular weight marker. **E**) Ubiquitination reactions in the presence of recombinant APC/C-pE or APC/C-pE-3A, which carries in addition alanine mutations at T119^{Apc4}, T178^{Apc5}, and S179^{Apc5}. Fluorescently labeled N-terminal domain of Cyclin B was analyzed by SDS-PAGE and fluorescence scanning. MCC containing BubR1$^{\Delta LL}$:Bub3 is less efficient in inhibiting Cyclin B ubiquitination by APC/C pE in comparison to MCC containing BubR1^{wt}:Bub3. The same pattern and level of inhibition is observed with APC/C-pE-3A, implying that the phosphomimetic mutation of these residues in APC/C pE does not contribute to MCC inhibition. NTD, N-terminal domain; Ub, ubiquitin.

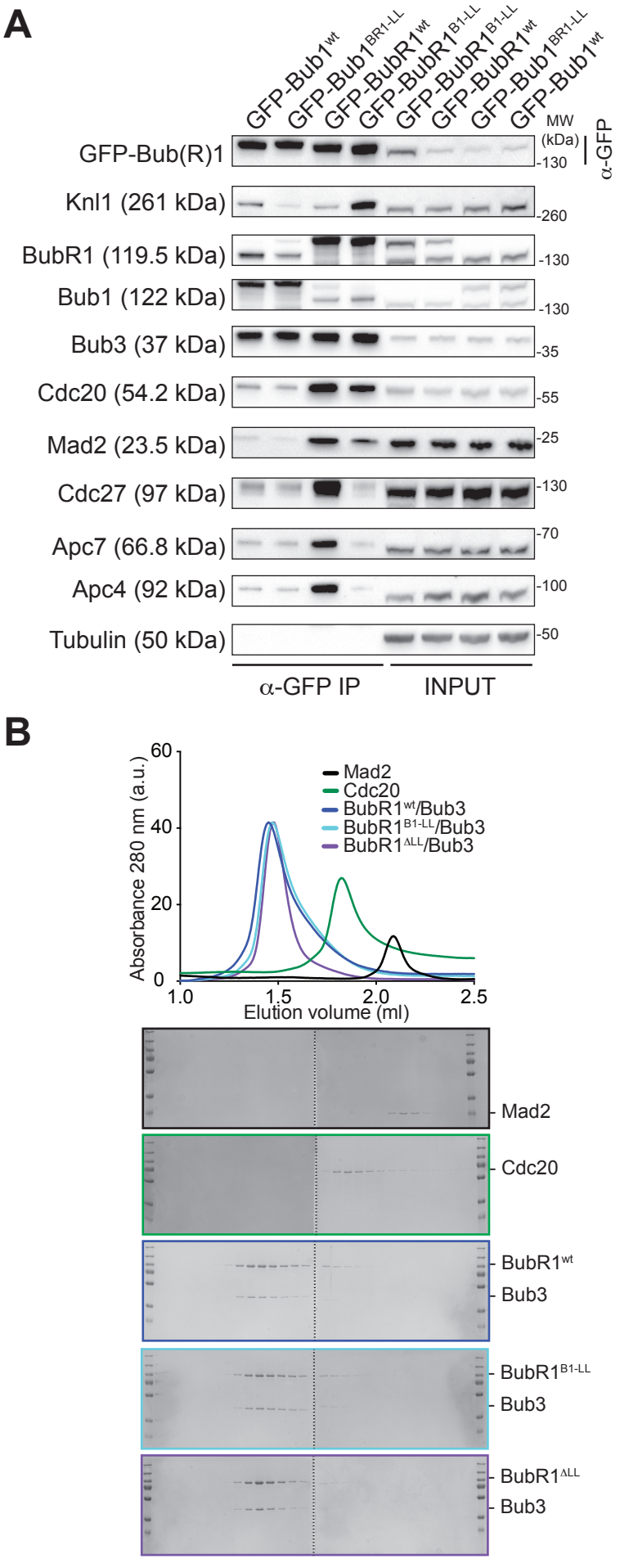
A
GFP-Bub1wt
GFP-Bub1BR1-LL
GFP-BubR1wt
GFP-BubR1B1-LL
GFP-BubR1B1-LL
GFP-BubR1wt
GFP-Bub1BR1-LL
GFP-Bub1wt
MW (kDa)
α-GFP
GFP-Bub(R)1
-130
Knl1 (261 kDa)
-260
BubR1 (119.5 kDa)
-130
Bub1 (122 kDa)
-130
Bub3 (37 kDa)
-35
Cdc20 (54.2 kDa)
-55
Mad2 (23.5 kDa)
-25
Cdc27 (97 kDa)
-130
Apc7 (66.8 kDa)
-70
Apc4 (92 kDa)
-100
Tubulin (50 kDa)
-50
α-GFP IP
INPUT
B
Absorbance 280 nm (a.u.)
60
40
20
0
1.0
1.5
2.0
2.5
Elution volume (ml)
Mad2
Cdc20
BubR1wt/Bub3
BubR1B1-LL/Bub3
BubR1ΔLL/Bub3
Mad2
Cdc20
BubR1wt
Bub3
BubR1B1-LL
Bub3
BubR1ΔLL
Bub3

Figure S7 ***Bub1$^{BR1\text{-}LL}$ does not bind APC/C effectively.*** **Related to Figures 4 and 5.** **A**) Western Blot of immunoprecipitates (IP) from mitotic Flp-In T-REx cell lines expressing the indicated GFP-Bub1 and GFP-BubR1 constructs showing that BubR1$^{B1\text{-}LL}$ shows impaired APC/C binding but Bub1$^{BR1\text{-}LL}$ does not show improved binding to APC/C. **B**) Control chromatograms for the individual components of the MCC complexes shown in Figure 5A. The height of the curves for the three different BubR1:Bub3 complexes was rescaled to match that of BubR1^{wt}:Bub3. All BubR1 proteins consist of residues 1-571 (a SAC proficient truncation mutant) and are N-terminally tagged with mTurquoise. a.u., arbitrary units.

Table S1 ***Summary of FRAP data analysis.*** **Related to Figures 1-3.**

Construct	RNAi depletion	$t_{1/2}$ (s)	Recovery (%)	R^2	Model preferred by Prism
GFP-BubR1^{wt}	BubR1	7.7	87	0.63	1-phase
GFP-BubR1$^{B1\text{-}LL}$	BubR1	5.2 (15.5%) 56.4 (84.5%)	119	0.80	2-phase
GFP-BubR1$^{B1\text{-}LL}$	Bub1	10.8	96	0.62	1-phase
GFP-Bub1^{wt}	Bub1	11.6	90	0.71	1-phase
GFP-BubR1$^{B1\text{-}B3BD/B1\text{-}H}$	BubR1	11.2	92	0.65	1-phase
GFP-BubR1$^{B1\text{-}LL/\Delta H}$	BubR1	6.6	92	0.60	1-phase
GFP-BubR1$^{\Delta LL}$	BubR1	9.9	92	0.61	1-phase

Supplemental References

S1. Primorac, I., Weir, J.R., Chiroli, E., Gross, F., Hoffmann, I., van Gerwen, S., Ciliberto, A., and Musacchio, A. (2013). Bub3 reads phosphorylated MELT repeats to promote spindle assembly checkpoint signaling. Elife *2*, e01030.

S2. Overlack, K., Primorac, I., Vleugel, M., Krenn, V., Maffini, S., Hoffmann, I., Kops, G.J., and Musacchio, A. (2015). A molecular basis for the differential roles of Bub1 and BubR1 in the spindle assembly checkpoint. Elife *4*.

S3. Taylor, S.S., Ha, E., and McKeon, F. (1998). The human homologue of Bub3 is required for kinetochore localization of Bub1 and a Mad3/Bub1-related protein kinase. J Cell Biol *142*, 1-11.

S4. Krenn, V., Wehenkel, A., Li, X., Santaguida, S., and Musacchio, A. (2012). Structural analysis reveals features of the spindle checkpoint kinase Bub1-kinetochore subunit Knl1 interaction. J Cell Biol *196*, 451-467.

S5. Faesen, A.C., Thanasoula, M., Maffini, S., Breit, C., Muller, F., van Gerwen, S., Bange, T., and Musacchio, A. (2017). Basis of catalytic assembly of the mitotic checkpoint complex. Nature *542*, 498-502.